FECONDAZIONE

Figure 2. Model of sperm guidance and selection within the oviduct. The fraction of spermatozoa reaching the uterus ...

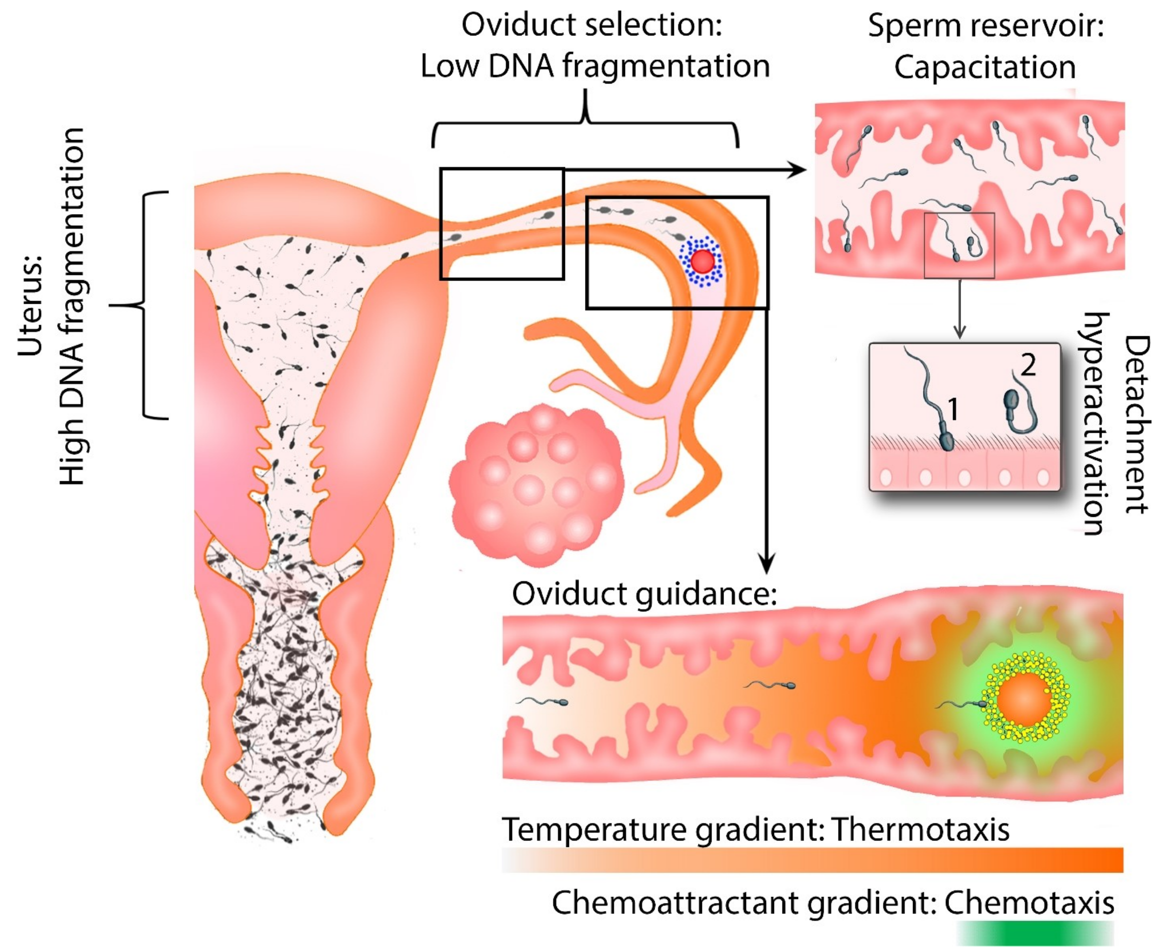

Biol Reprod, Volume 98, Issue 3, March 2018, Pages 262–276, https://doi.org/10.1093/biolre/iox173

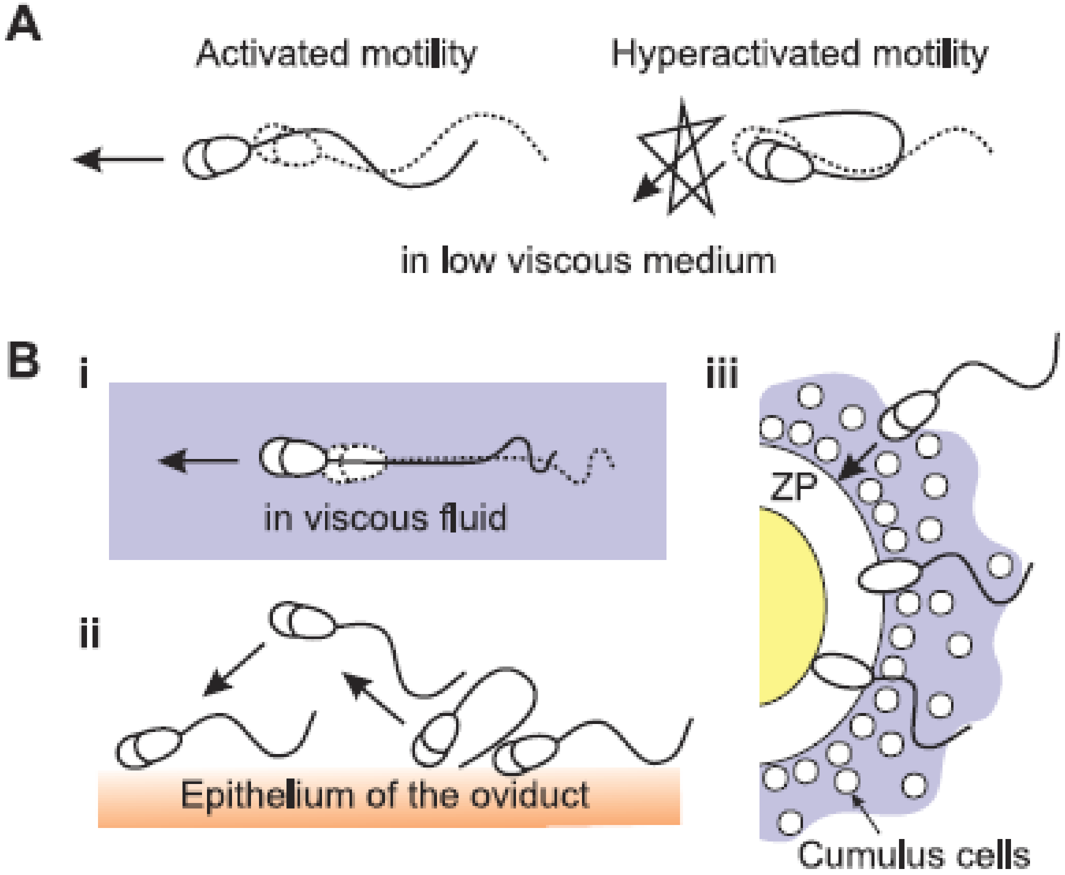

FIGURE 4. Properties and physiological roles of hyperactivation. *A*: activated (*left*) and hyperactivated (*right*) flagellar shape and motility direction (arrows) displayed by spermatozoa in nonviscous experimental media. Activated spermatozoa advance showing a symmetric flagellar bend, while hyperactivated spermatozoa tumble in one place and do not advance efficiently due to an asymmetric flagellar beating pattern. *B*: importance of hyperactivated sperm motility: *i*) To advance in highly viscoelastic fluids in the female genital tract more effectively than activated sperm, *ii*) to detach spermatozoa from the isthmus reservoir and advance towards the ampulla (site of fertilization), and *iii*) to facilitate sperm penetration through the cumulus matrix and the zona pellucida.

Detachment from tubal epithelium

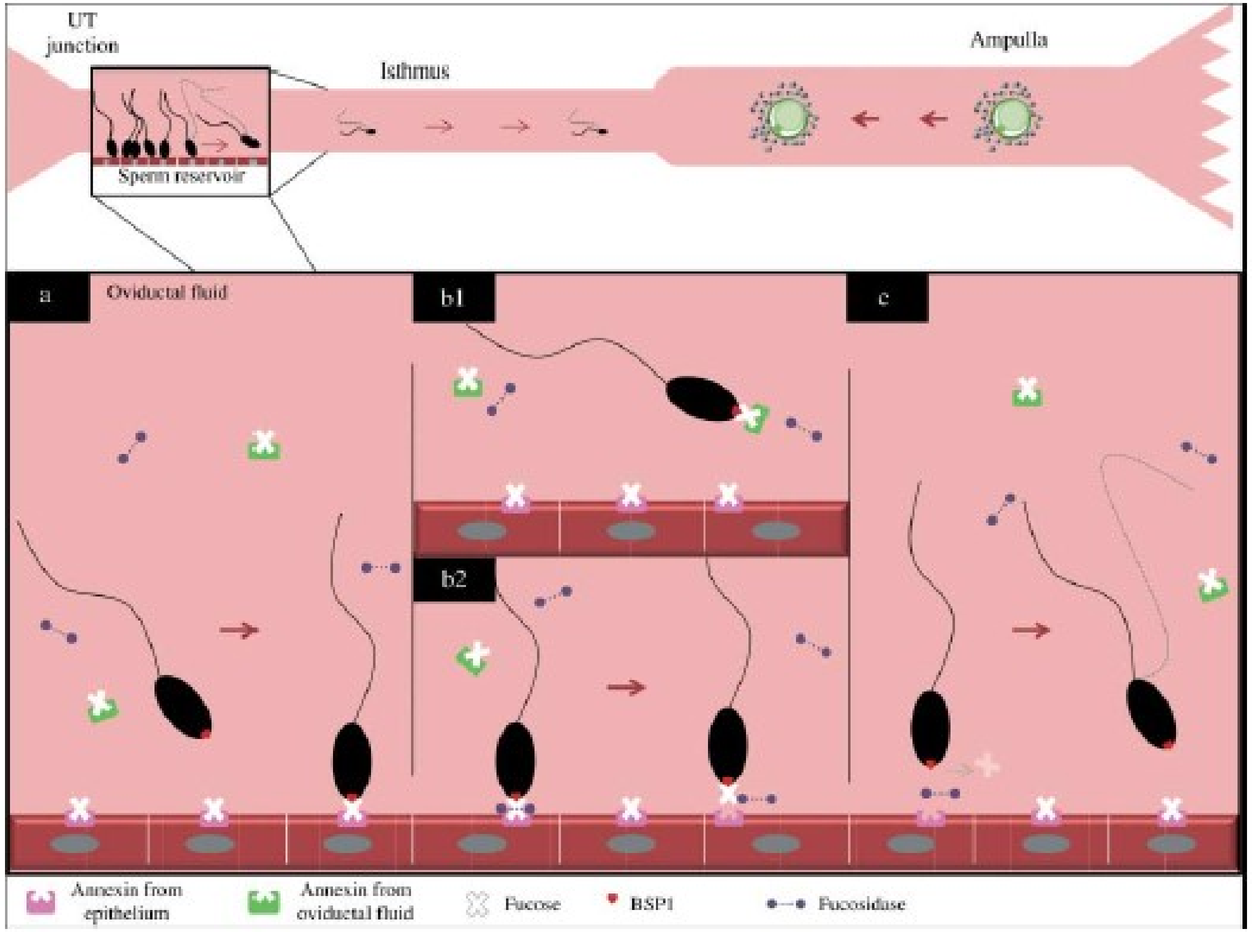

Figure 1 Mechanism for the sperm binding and releasing from the oviduct in the bovine model. (a) Sperm binding is mediated by lectin-like protein as BSP1 present in the sperm plasma membrane that recognizes fucose contained in the annexin molecule bound to the epithelial cell membrane. (b) Sperm binding to the oviduct could be modulated by two different mechanisms that can act at the same time. (b1) Annexin present in the oviductal fluid compete for the BSP1 binding site present on the sperm. (b2) Fucosidase enzymes present in the oviductal fluid can remove fucose residues contained in the annexin present in the oviductal epithelium. (c) These different mechanisms and the development of hyperactivative motility allow the sperm release from the oviductal reservoir.

fecondazione

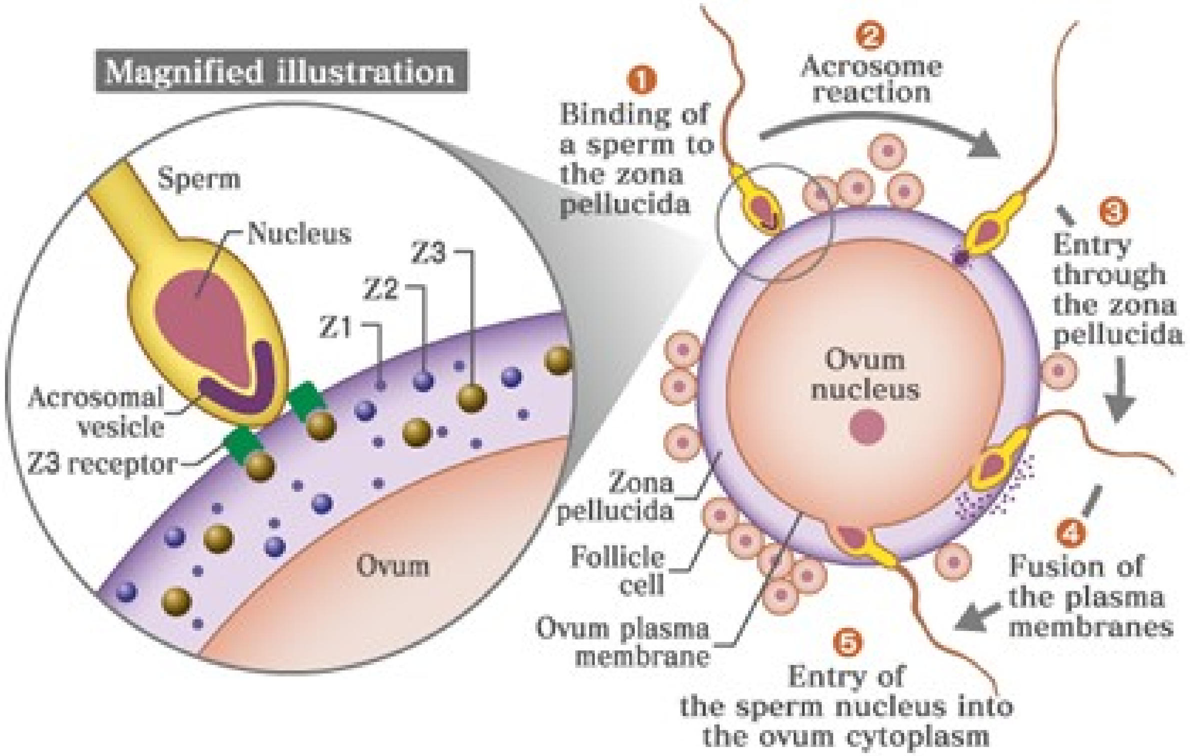

+ ZOOM

Reazione acrosomiale

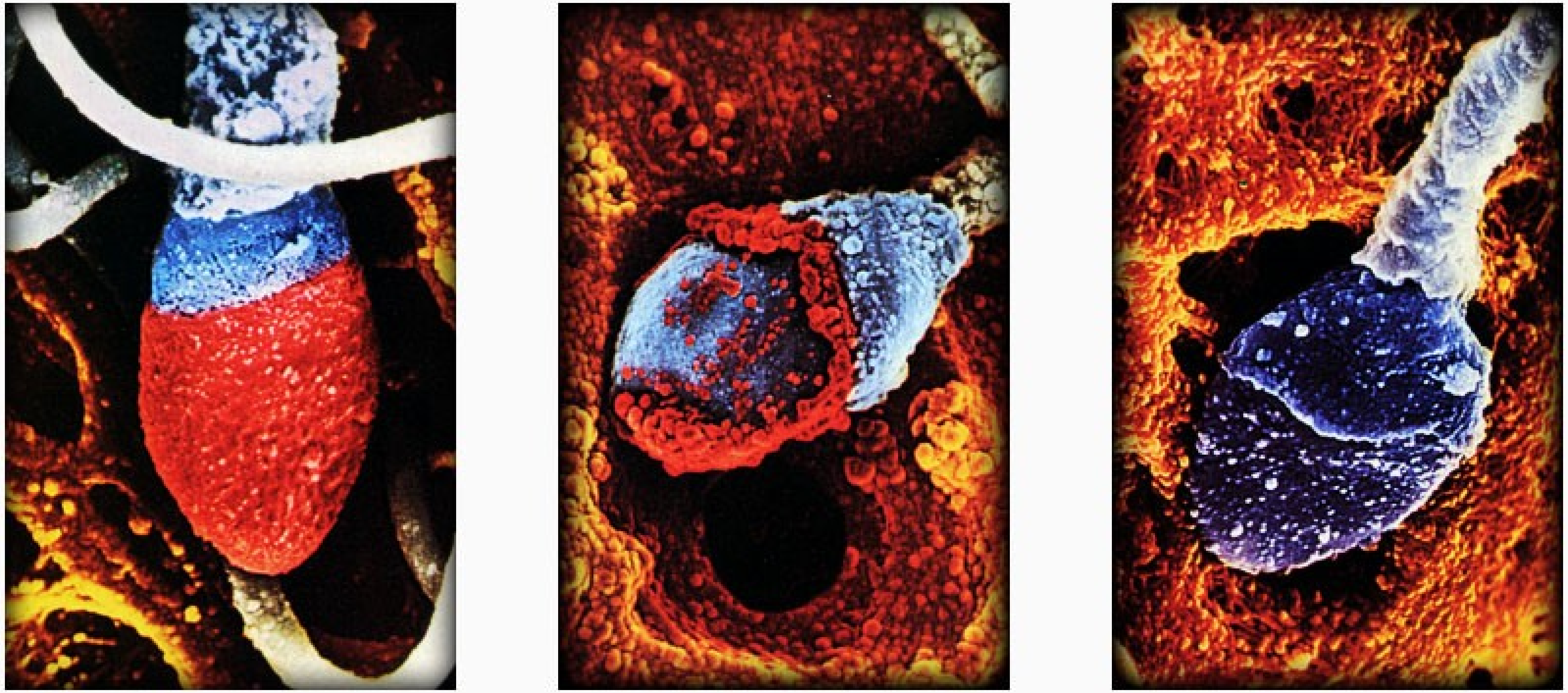

Acrosome reaction

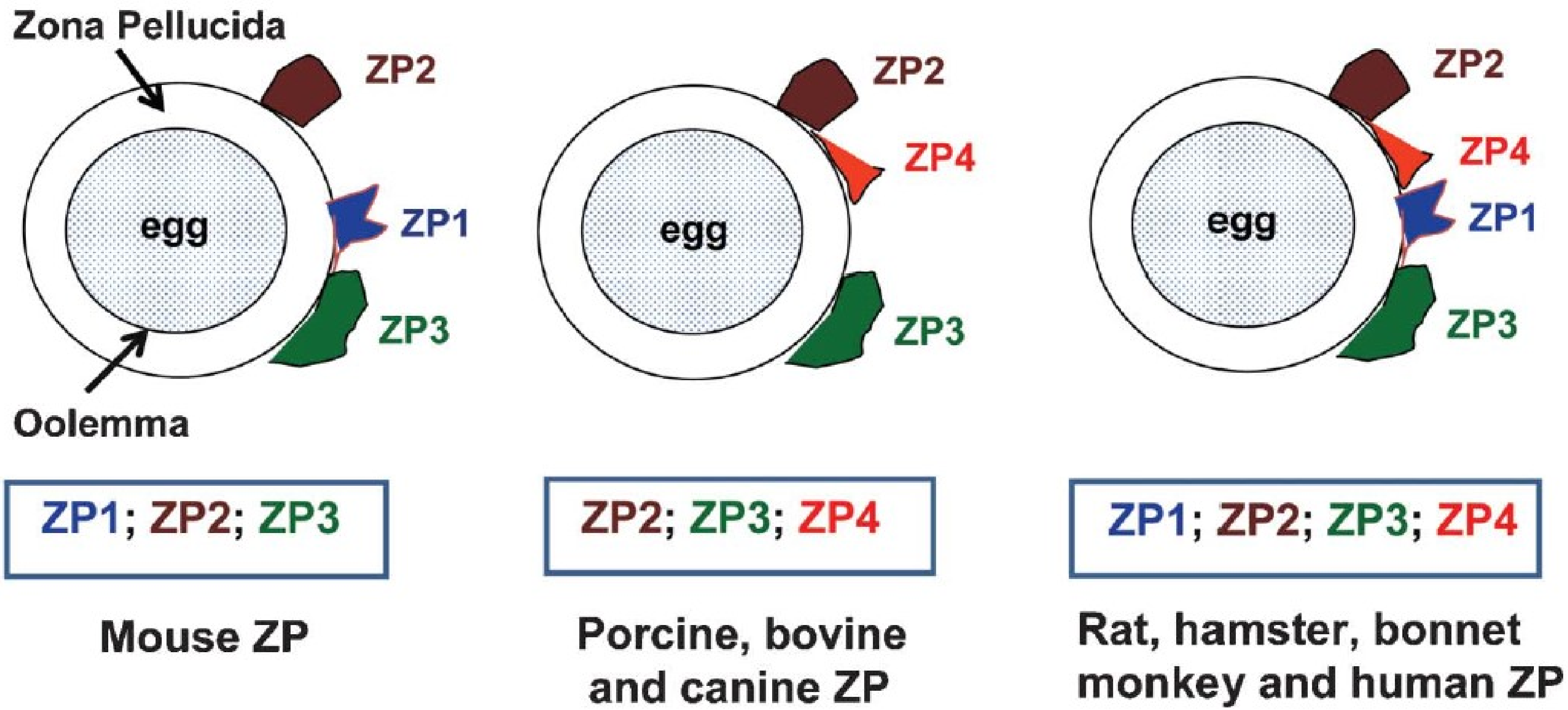

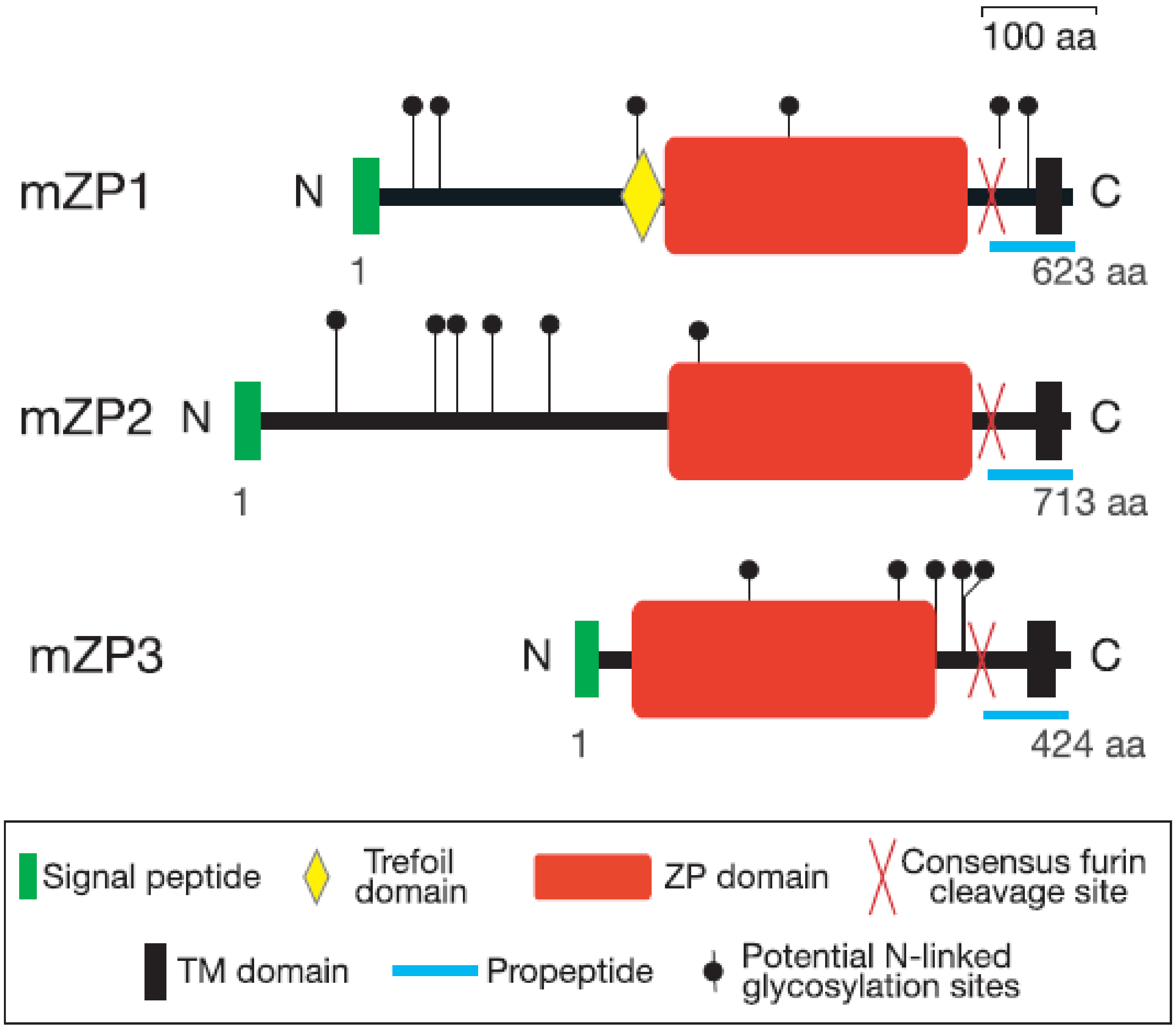

100 aa
mZP1
N
C
1
623 aa
mZP2
N
C
1
713 aa
mZP3
N
C
1
424 aa
Signal peptide
Trefoil domain
ZP domain
Consensus furin cleavage site
TM domain
Propeptide
Potential N-linked glycosylation sites

ZP3

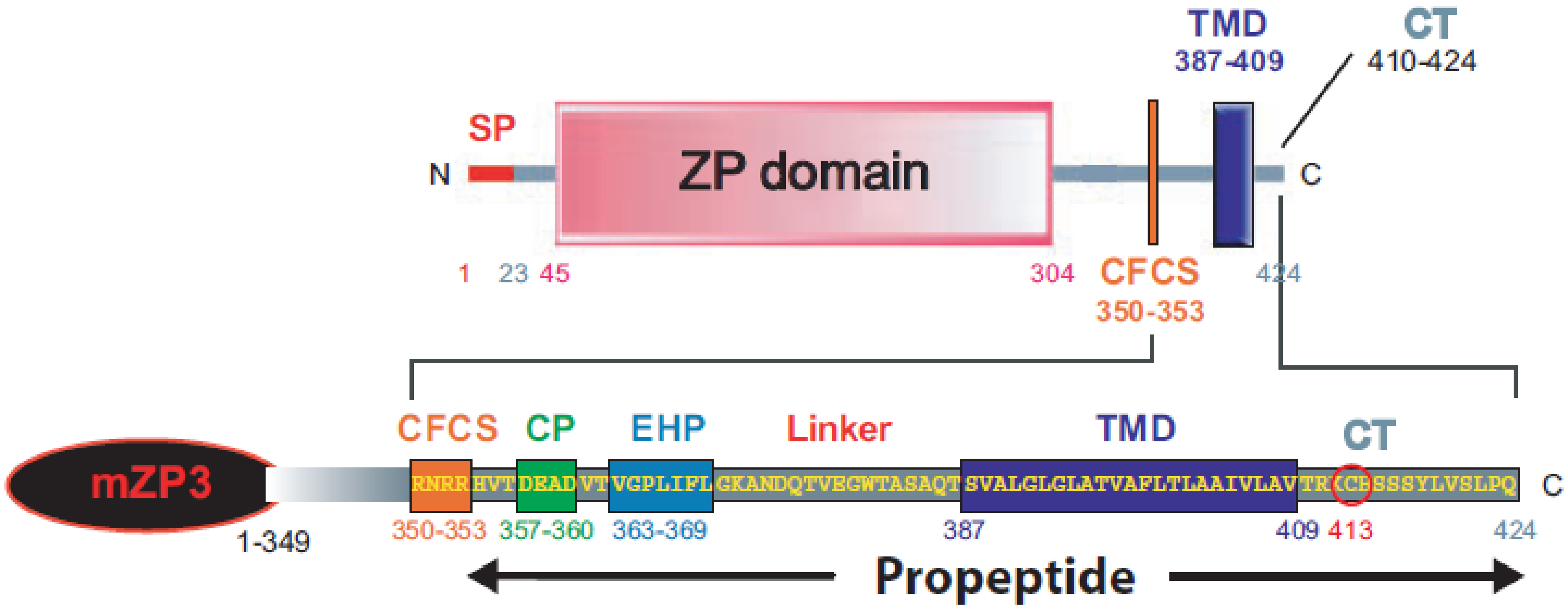
TMD
387-409
CT
410-424
SP
N
ZP domain
C
1
23
45
304
CFCS
350-353
424
CFCS
CP
EHP
Linker
TMD
CT
mZP3
RNRR HVT DEAD VT VGPLIFL GKANDQTVEGWTASAQT SVALGLGLATVAFLTLAAIVLAV TRKCHSSSYLVSLPQ
C
1-349
350-353
357-360
363-369
387
409
413
424
Propeptide

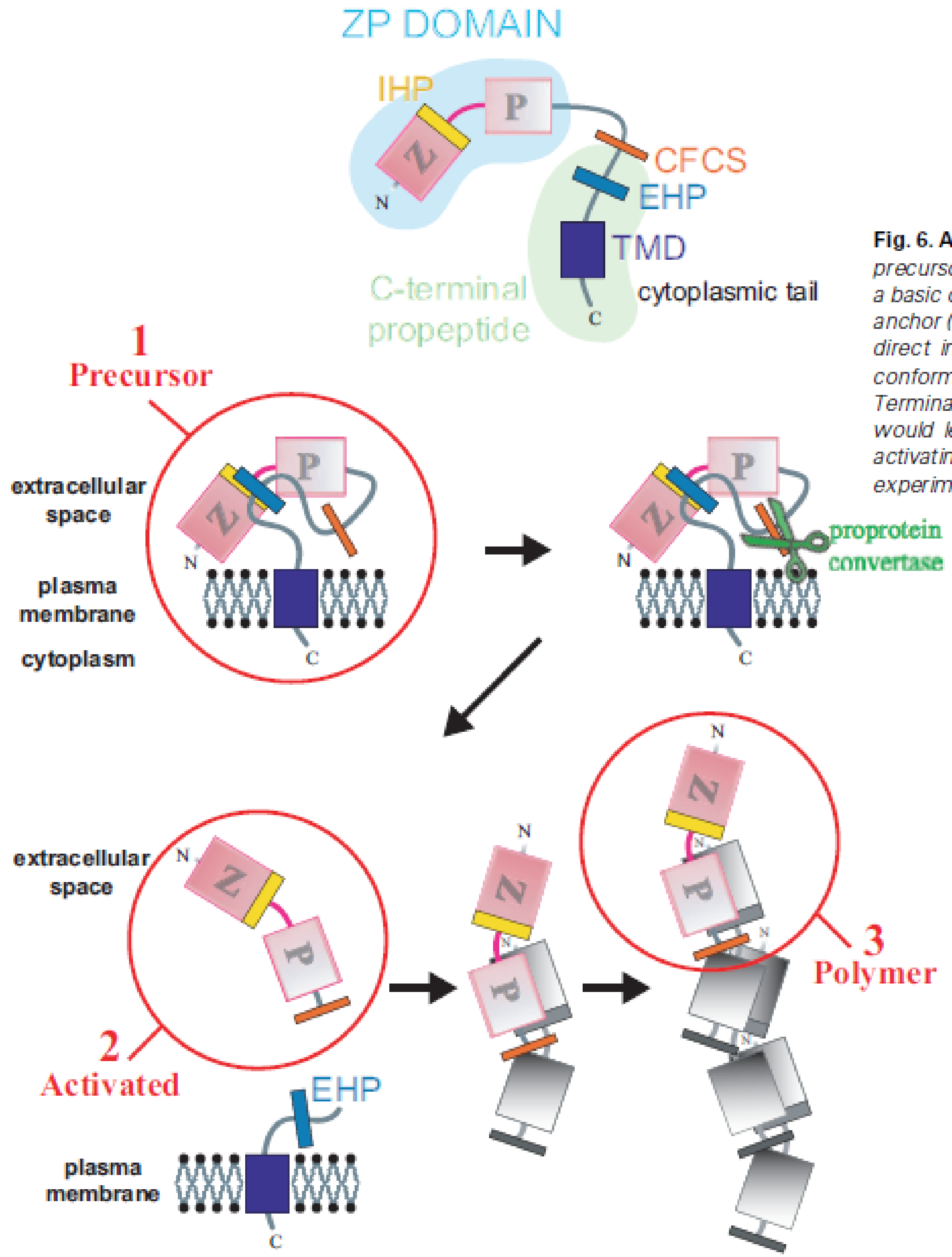

Fig. 6. A general mechanism for assembly of ZP domain proteins. *In all ZP domain precursors, the ZP domain is followed by a C-terminal propeptide (CTP) that contains a basic cleavage site (such as a CFCS), and EHP, and, in most cases, a TMD or GPI-anchor (top panel). Precursors do not polymerize within the cell either as a result of direct interaction between the EHP and IHP or because they adopt an inactive conformation dependent on the presence of both patches (middle left panel). C-Terminal processing at the CFCS by a proprotein convertase (middle right panel) would lead to dissociation of mature proteins from the EHP (bottom left panel), activating them for assembly into filaments and matrices (bottom right panel). For experimental details that led to this mechanism see Jovine* et al. *(2004).*

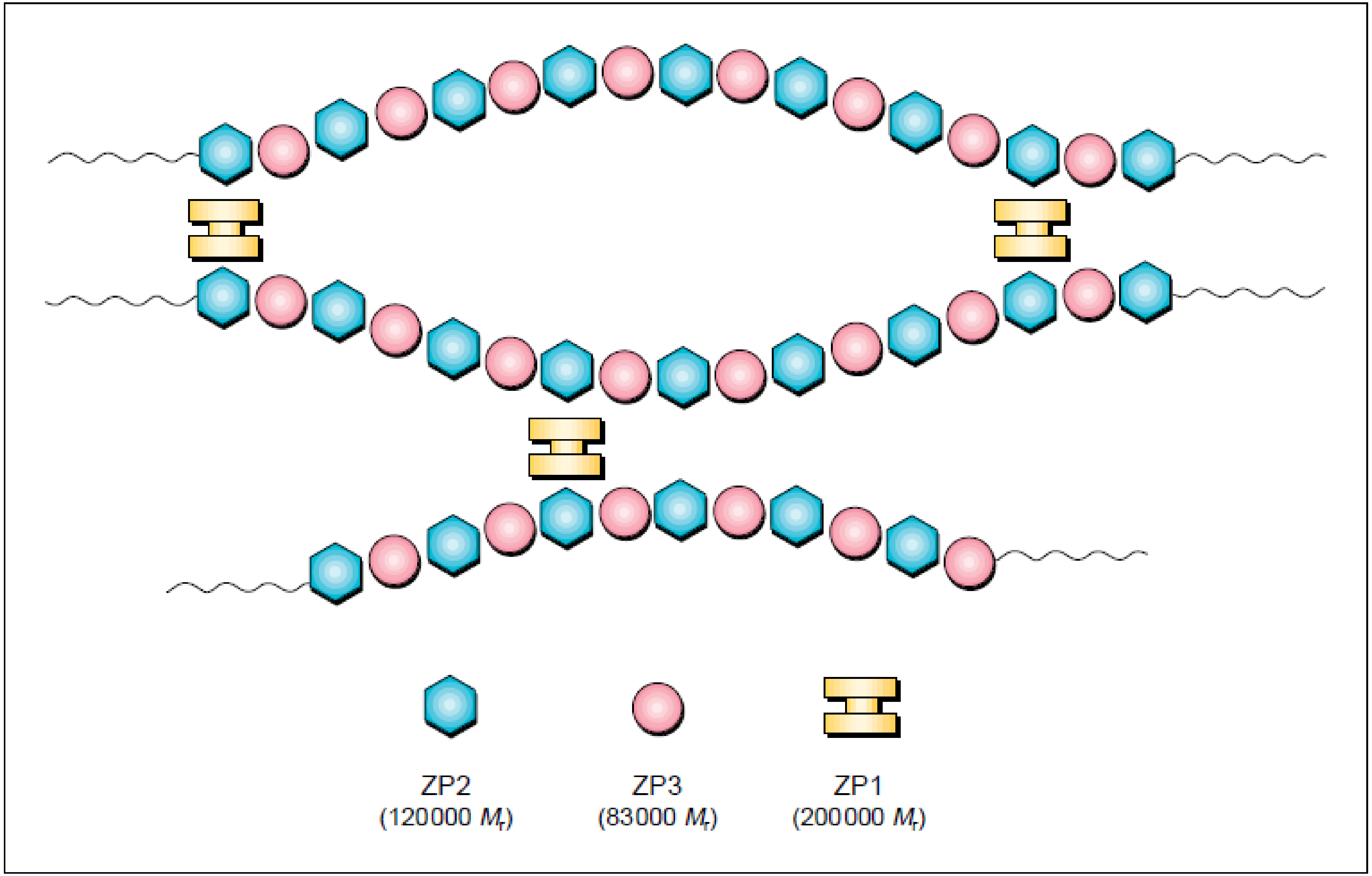

Fig. 1. The current model of the zona pellucida as proposed by Wassarman and redrawn from Wassarman (1988). Filaments are constructed of repeating ZP2–ZP3 units and are cross-linked by ZP1. Calculations of the ZP2:ZP3 ratio using recent sequence data confirm that it is close to 1:1. Although the model is consistent with experimental observations, formal proof that the zona pellucida is constructed in this way is still lacking. It is unclear whether ZP1 binding sites are present on every ZP2–ZP3 dimer and, if so, how ZP1 cross-links are actually distributed.

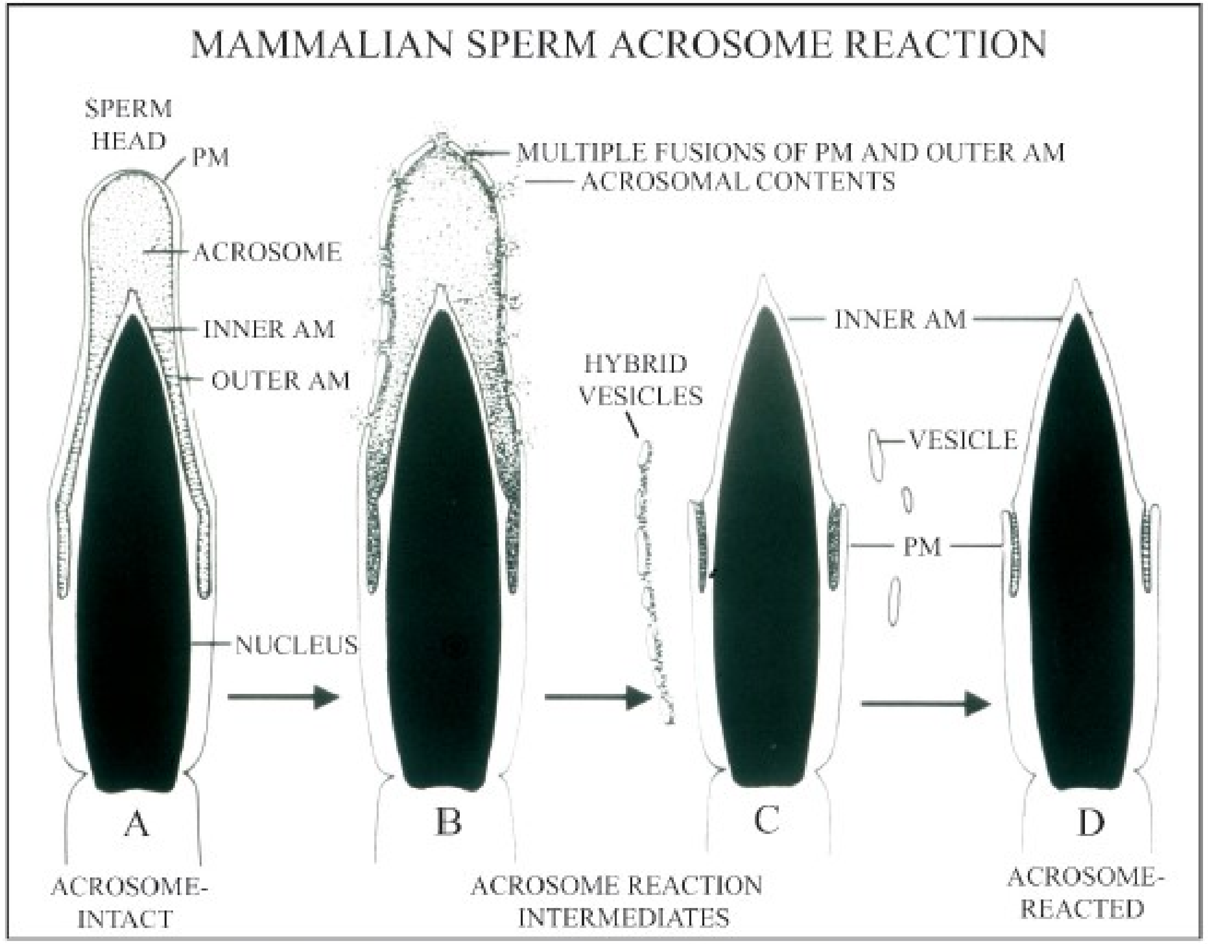

ZP3 stimulates several signal-transducing components in sperm, including: G proteins, IP3 and IP3 receptors, phospholipase C, voltage sensitive calcium channels.

- Activates G proteins (Gi1, Gi2, Gq/11)
- Depolarizes plasma membrane (-60 to -30 mV)
- Increases intracellular pH (by 0.3 units)
- Increases intracellular [calcium] (from 150 to 400 nM)

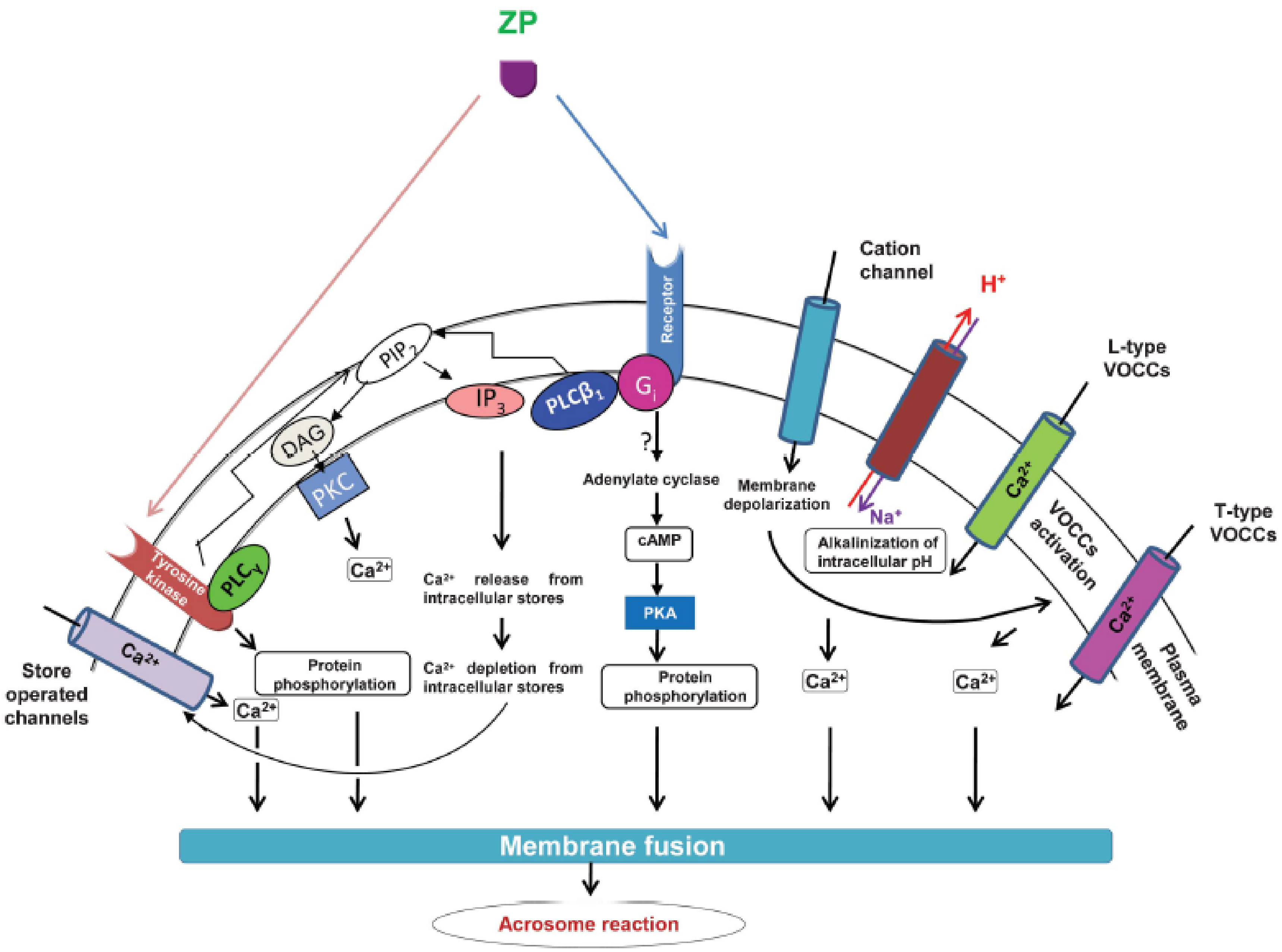
ZP
Receptor
Cation channel
H+
L-type VOCCs
T-type VOCCs
PIP2
IP3
PLCβ1
Gi
DAG
PKC
?
Adenylate cyclase
Membrane depolarization
Na+
Alkalinization of intracellular pH
VOCCs activation
Ca2+
Tyrosine kinase
PLCγ
Ca2+ release from intracellular stores
cAMP
PKA
Store operated channels
Protein phosphorylation
Ca2+ depletion from intracellular stores
Protein phosphorylation
Plasma membrane
Membrane fusion
Acrosome reaction

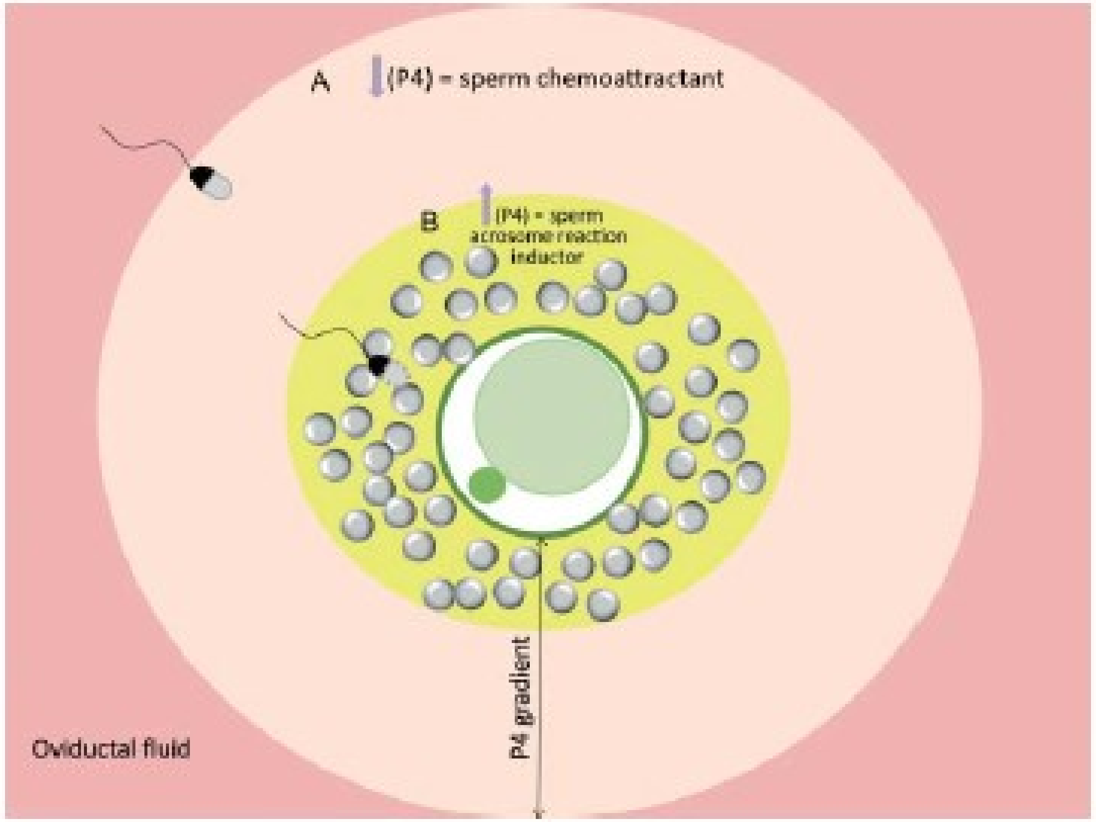

Figure 5 Progesterone (P_4) levels close to the fertilization location and its effect on sperm. (A) Low P_4 levels acting like a chemoattractant driving the sperm toward the oocyte. (B) High P_4 levels secreted by cumulus cells induce acrosome reaction.

Membrane depolarization

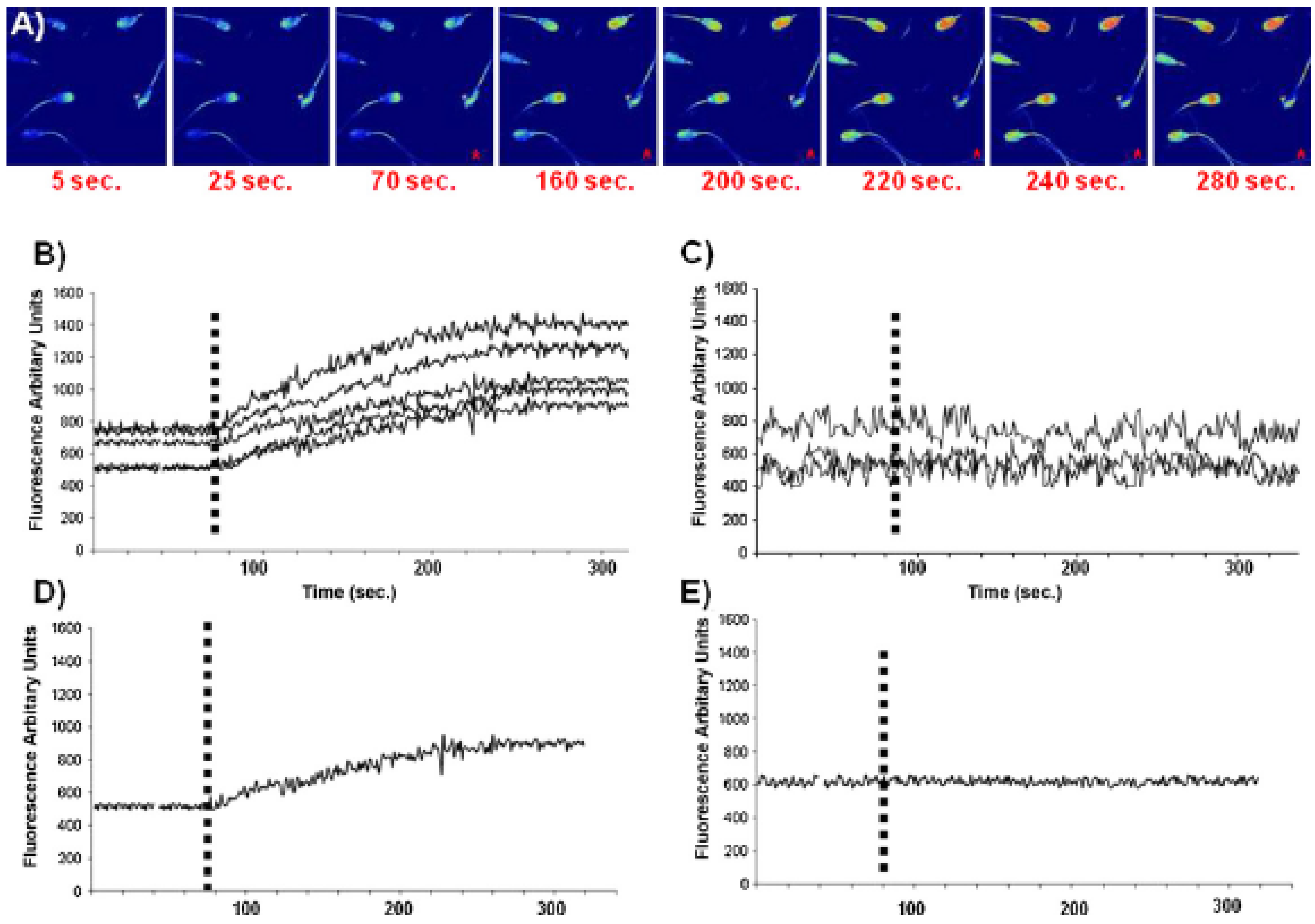

Calcium peack

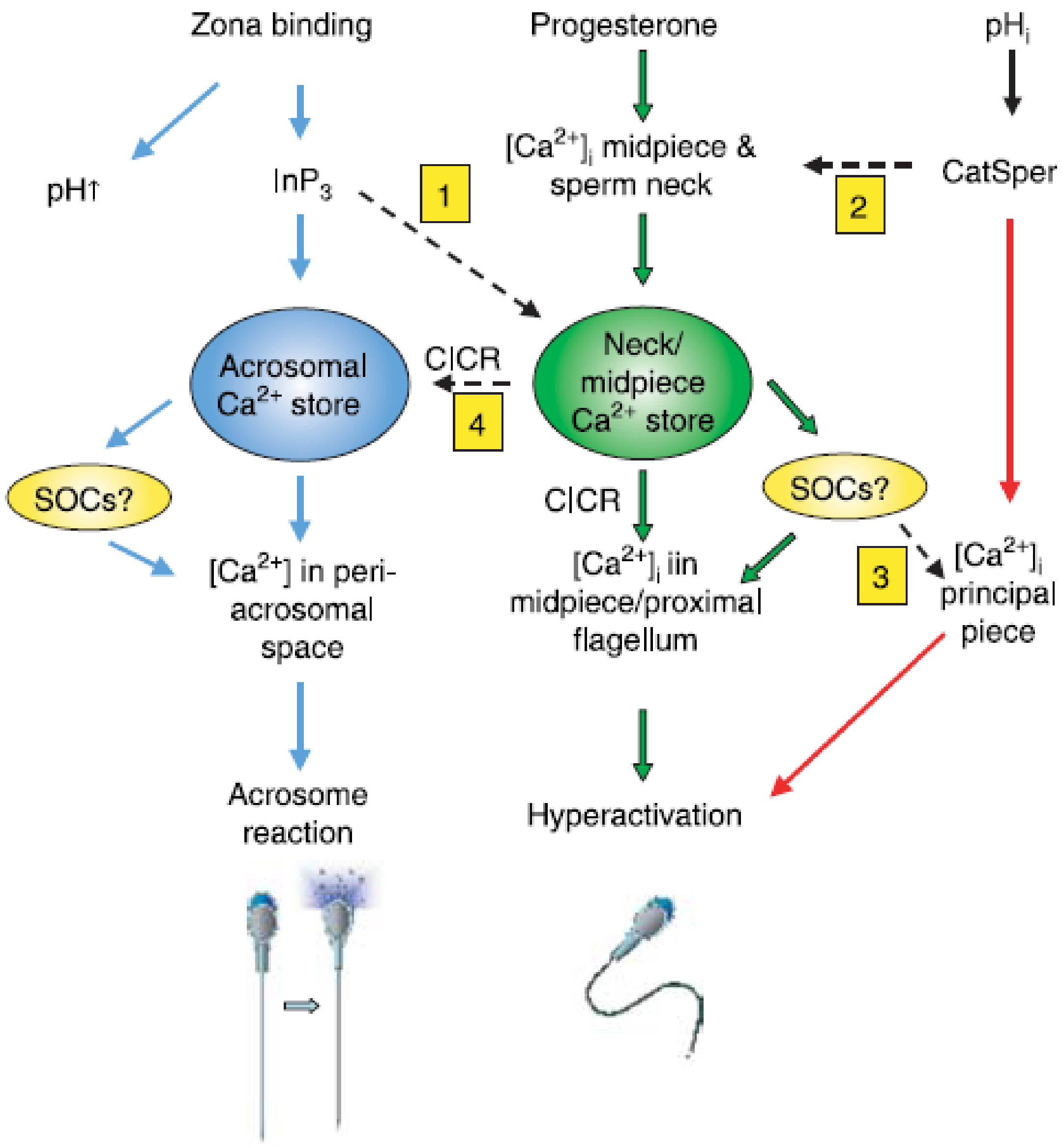

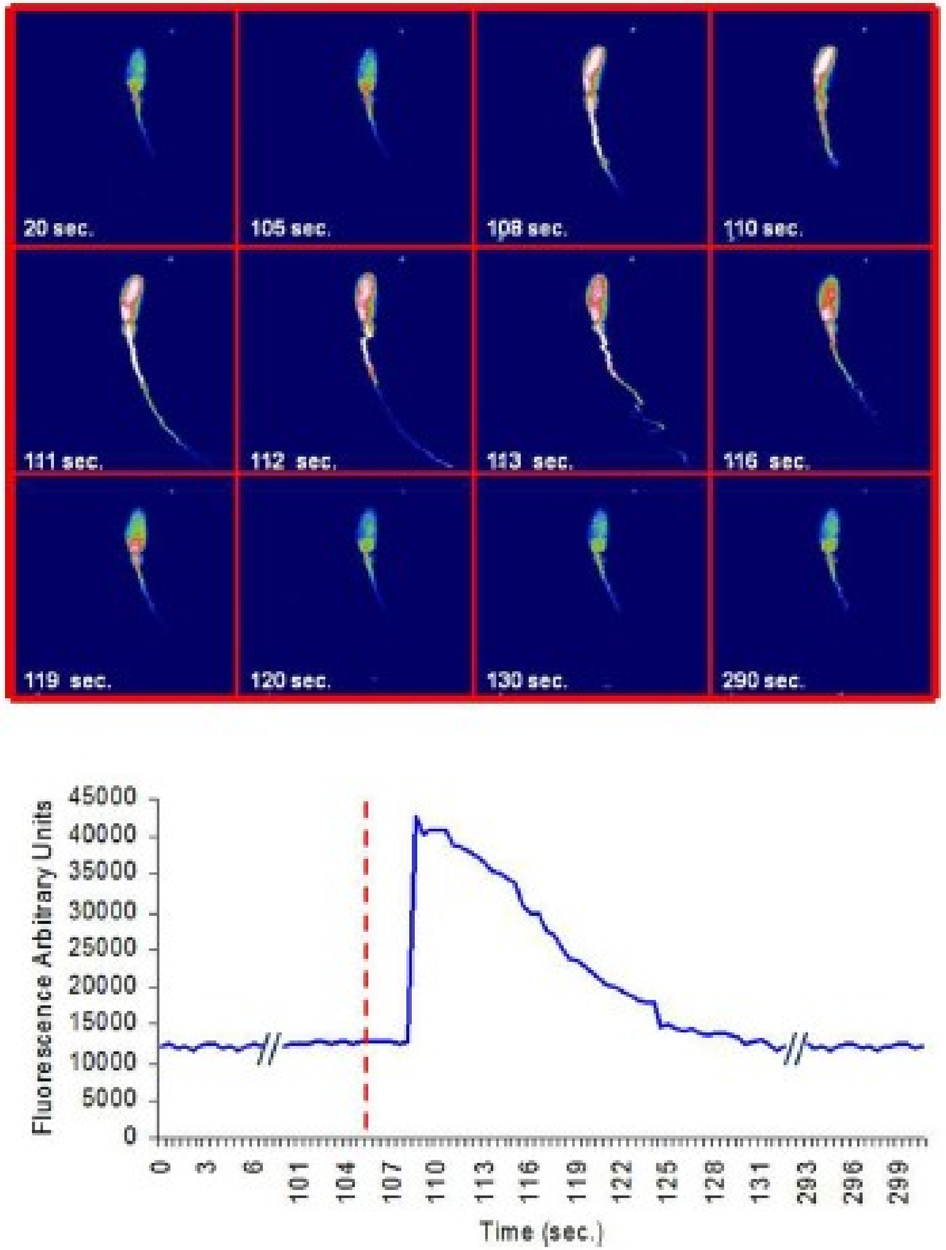

Figure 9 An example of confocal image gallery of CD treated spermatozoa loaded with Fluo-3AM exposed to sZP. An example of confocal image gallery of CD treated spermatozoa loaded with Fluo-3AM exposed to sZP (vertical red line). Notice that the rise in the $[Ca^{2+}]_i$ in spermatozoon is evident after <10 sec. from sZP addition, whereas return on the baseline occurs after about 30 sec.

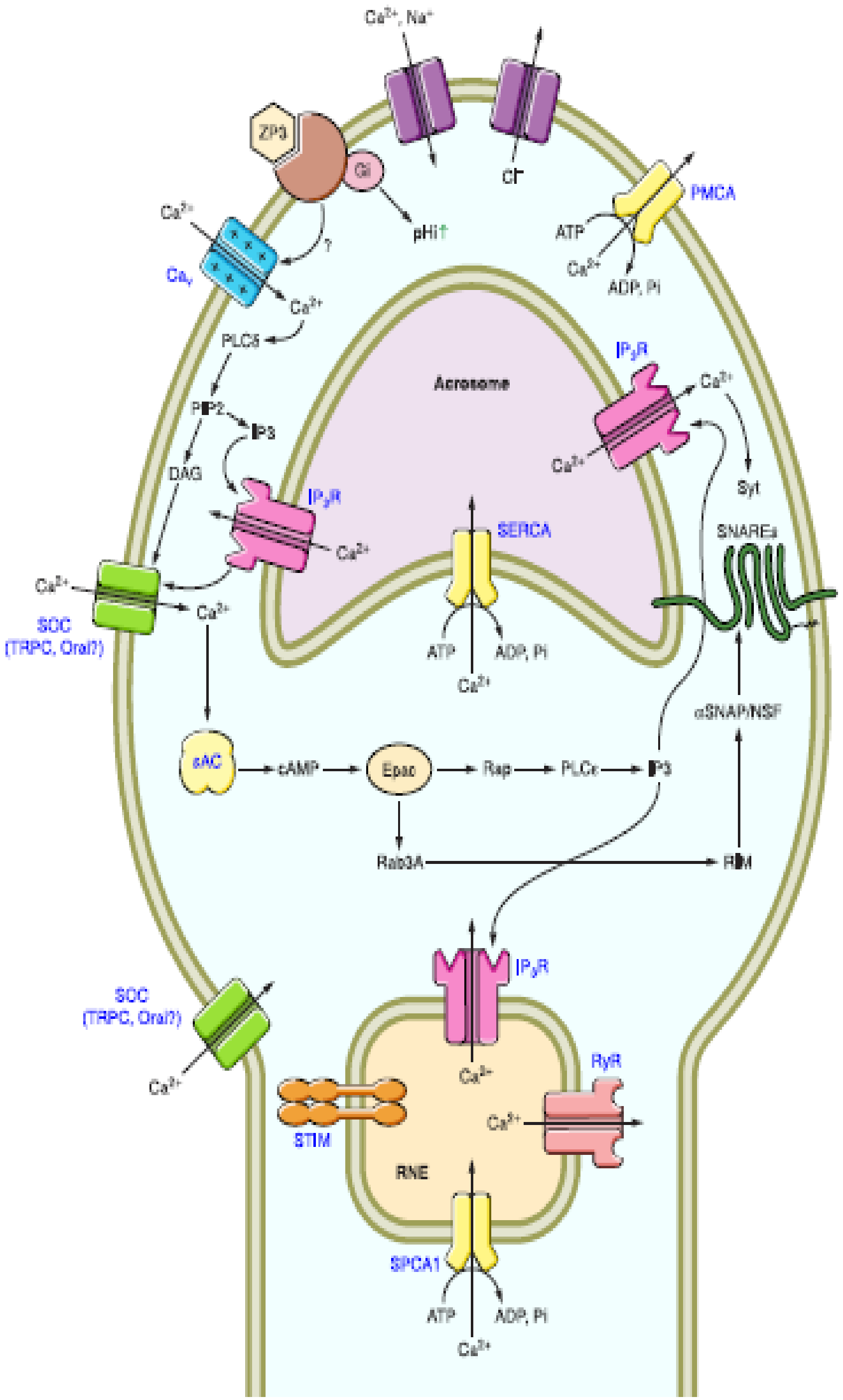

Ca2+, Na+
Cl⁻
ZP3
Gi
pHi↑
PMCA
ATP
Ca2+
ADP, Pi
Ca2+
?
Cav
Ca2+
PLCδ
PIP2
IP3
DAG
IP3R
Ca2+
Acrosome
IP3R
Ca2+
Ca2+
Syt
SERCA
SNAREs
Ca2+
SOC
(TRPC, Orai?)
Ca2+
ATP
ADP, Pi
Ca2+
αSNAP/NSF
sAC
cAMP
Epac
Rap
PLCε
IP3
Rab3A
RIM
IP3R
SOC
(TRPC, Orai?)
Ca2+
Ca2+
RyR
Ca2+
STIM
RNE
SPCA1
ATP
ADP, Pi
Ca2+